Study of Si4 and Si4 − using threshold photodetachment (ZEKE) spectroscopy

Caroline C. Arnold and Daniel M. Neumark

Citation: The Journal of Chemical Physics **99**, 3353 (1993); doi: 10.1063/1.465145
View online: http://dx.doi.org/10.1063/1.465145
View Table of Contents: http://scitation.aip.org/content/aip/journal/jcp/99/5?ver=pdfcov
Published by the AIP Publishing

Study of Si_4 and Si_4^- using threshold photodetachment (ZEKE) spectroscopy

Caroline C. Arnold and Daniel M. Neumark[a)]
Department of Chemistry, University of California, Berkeley, California 94720 and Chemical Sciences Division, Lawrence Berkeley Laboratory, Berkeley, California 94720

(Received 19 April 1993; accepted 24 May 1993)

The threshold photodetachment (ZEKE) spectrum of Si_4^- is presented. Although no transitions to the ground state of Si_4 are observed, we obtain detailed information on the anion and several of the low-lying excited states of neutral Si_4. The spectrum shows a long progression of well-resolved transitions between the D_{2h} $^2B_{2g}$ rhombus anion and ν_2 vibrational levels of the first excited D_{2h} $^3B_{3u}$ neutral. The length and spacing of the progression is consistent with *ab initio* calculations performed by Rohlfing and Raghavachari [J. Chem. Phys. **96**, 2114 (1992)], but some of the sequence bands observed within the progression are not. We also observe transitions to the Si_4 $^1B_{3u}$ state which is found at a lower excitation energy than predicted. The perturbed vibrational structure in this band is attributed to vibronic coupling to a nearby electronic state which is "dark" with respect to ZEKE spectroscopy. The ZEKE spectra are compared to the previously obtained photoelectron spectra of Si_4^- as well as *ab initio* calculations on Si_4^- and Si_4.

I. INTRODUCTION

The study of small silicon clusters has been an area of interest because of their importance in astrophysics[1] and CVD processes.[2] These species are of considerable interest from a purely spectroscopic perspective as well, since *ab initio* calculations[3–5] predict dramatic changes in the geometry and bonding in silicon clusters as the number of atoms is varied. However, from an experimental viewpoint, the spectroscopy of silicon clusters is quite poorly characterized with the exception of the dimer,[6] for which several rotationally resolved electronic transitions have been observed. The development of laser vaporization cluster sources has facilitated photofragmentation,[7] photoionization,[8] and "reactive etching" studies,[9] of the larger clusters, but these experiments have revealed little regarding specific cluster structures and bonding. Several absorption lines seen in silicon vapors trapped in rare gas matrices were tentatively attributed to Si_3 and Si_4, but no analysis of these lines was pursued.[10,11]

There have been several gas phase spectroscopic studies of silicon clusters with three or more atoms. With the exception of the emission spectroscopy study of Gole and co-workers,[12] in which several transitions from two excited electronic states attributed to Si_3 were observed, this work has involved negative ion photodetachment experiments on silicon cluster anions.[13–17] While the resolution obtained in photodetachment experiments is typically lower than ir absorption techniques, they offer the advantage of mass selection prior to spectroscopic investigation, thereby eliminating any ambiguity concerning species identification. Such experiments have also revealed a great deal about the electronic structure of metal clusters[18] and carbon clusters.[19]

Electronically resolved negative ion photoelectron spectra (PES) of Si_n^- (n=3–12) have been obtained by Smalley and co-workers.[14] Higher resolution PES have been measured by Ellison for Si_2^-,[15] and by our group for Si_2^-–Si_4^-.[16,17] These studies have shown that silicon clusters are rich with low-lying electronic states, and the higher resolution studies revealed vibrational structure associated with several of the neutral←anion electronic transitions. We have also studied Si_2^- at even higher resolution using threshold photodetachment (zero electron kinetic energy, or ZEKE[20]) spectroscopy.[16] The ZEKE spectrum exhibited fine structure due to spin–orbit splitting both in the anion and neutral dimer, and this proved invaluable in sorting the low-lying electronic states in Si_2^- and Si_2.

In the case of our Si_3^- and Si_4^- photoelectron spectra, even though vibrational structure is resolved in several of the bands, the assignment of the vibrational and electronic features is greatly facilitated by comparing the experimental spectra to the *ab initio* work of Raghavachari, Rohlfing, and co-workers.[3,4] For example, their calculations on Si_4 and Si_4^- predicted the ground states to be the ^1A_g and the $^2B_{2g}$ states, respectively, both of which have planar rhombus (D_{2h}) structures. Based on the calculated geometries, which are quite similar, one would expect to see a short progression in the ν_2 mode of Si_4 with a frequency of 357 cm^{-1}. This is consistent with the experimental spectra,[17] shown in Fig. 1, thereby supporting the *ab initio* geometries.

Rohlfing and Raghavachari[4] have also investigated the excited states of Si_4 with a rhombus (or near rhombus) equilibrium geometry. They determined that at least six electronic states accessible by detachment of the anion ground state ($^2B_{2g}$) lie within 2 eV of the neutral ground state, and assigned the three excited state bands in our spectrum (bands *A*, *B*, and *C*[17]) to transitions to the $^3B_{3u}$, ^3B_g, and $^3B_{1u}$ states of Si_4. They also raised the possibility of that one of the bands (band *B*) consisted of overlapping transitions other low lying excited states of Si_4. The band assignments according to Ref. 4 are indicated in Fig. 1.

[a)]NSF Presidential Young Investigator and Camille and Henry Dreyfus Teacher–Scholar.

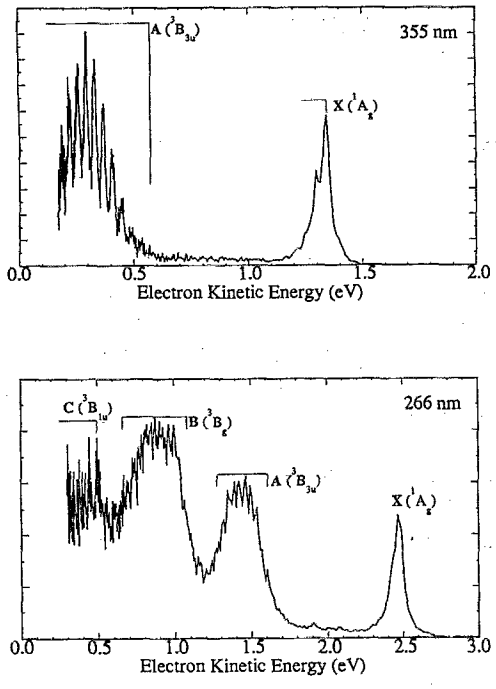

FIG. 1. Photoelectron spectra of Si_4^- (Ref. 17) obtained using 3.493 eV photon energy (top panel) and 4.66 eV photon energy (bottom panel) with the assignments of Rohlfing and Raghavachari (Ref. 4).

The partially resolved vibrational features in Fig. 1 suggest that a higher resolution photodetachment spectrum will reveal considerably more structure. This is the motivation for the work presented here, in which we report the results of threshold photodetachment (ZEKE) spectroscopy on Si_4^-. In these experiments, mass-selected anions are photodetached with a tunable laser, and only those electrons with nearly zero kinetic energy are detected. The resolution of our ZEKE spectrometer is around 3 cm^{-1}, considerably better than the photoelectron spectrometer used for Fig. 1 (80–100 cm^{-1}).

Threshold photodetachment spectroscopy is most powerful when used in tandem with photoelectron spectroscopy. While all neutral←anion electronic transitions involving removal of a single electron can be seen in the photoelectron spectrum of an anion, this is not so for the ZEKE spectrum. According to the Wigner[21] threshold law, the photodetachment cross section near the threshold for a neutral←anion transition goes as

$$\sigma \propto (E_{\text{photon}} - E_{\text{threshold}})^{l+1/2}, \tag{1}$$

where l is the photoelectron angular momentum. For $l=0$ (s wave) detachment, the cross section rises sharply above threshold, but for $l \geqslant 1$ (p wave, etc.) the cross section is very small near threshold. Hence, ZEKE spectroscopy of anions is sensitive only to s wave detachment. While sometimes inconvenient, this feature is often useful in assigning neutral←anion electronic transitions, since s-wave detachment can only result from removal of an electron from particular orbitals.[22] This type of analysis was used in our study of Si_2^- (Ref. 16) as well as in the work presented here.

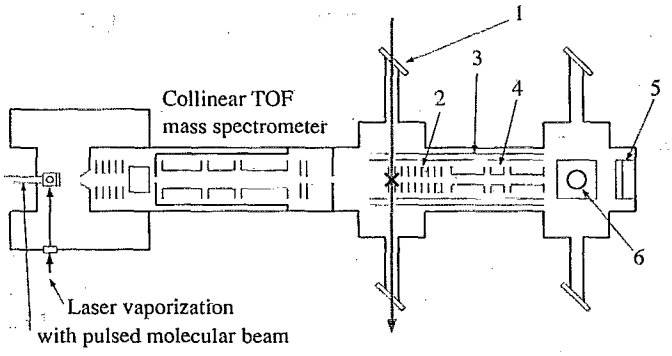

FIG. 2. Diagram of the tunable photodetachment apparatus: (×) interaction region; (1) detachment laser windows; (2) extraction plates and appertures; (3) magnetic shielding; (4) electron einzel lens; (5) ion detector (6) electron detector (above the plane).

The Si_4^- threshold photodetachment spectrum shows well resolved bands involving transitions between the Si_4^- $^2B_{2g}$ state and two excited electronic states of neutral Si_4. The lower energy band, assigned to the transition to the Si_4 $^3B_{3u}$ state, is particularly clean, and from it we obtain several vibrational frequencies for the anion and neutral which are in partial agreement with the *ab initio* results of Rohlfing and Raghavachari.[4] The higher energy band appears to be strongly perturbed, most likely because of vibronic coupling to an overlapping Si_4 excited state which is "dark" with respect to ZEKE spectroscopy. The nature of the electronic states that are involved in this band is discussed in light of the *ab initio* calculations.

II. EXPERIMENT

Figure 2 shows a schematic top view of the threshold photodetachment apparatus. It is described in detail elsewhere,[23] but the basic operation is as follows. Cold silicon clusters (anions, cations, and neutrals) are generated in a laser vaporization/pulsed molecular beam source similar to that developed by Smalley.[24] Helium is used as the carrier gas, typically with a backing pressure between 50 and 80 psi. Use of a piezoelectric valve[25] rather than the solenoid-type molecular beam valve (General Valve) used in previous cluster studies was found to greatly enhance cluster cooling. Laser vaporization is achieved by focusing a 2 mJ, 532 nm pulse from a frequency-doubled Nd:YAG laser (20 Hz repetition rate) onto a rotating, translating silicon rod. The negative ions that pass through a 2 mm diameter skimmer are collinearly accelerated to 1 keV. Mass selection is achieved by a 1 m long beam-modulated time-of-flight mass spectrometer. The mass separated ions then enter the detector region where they are photodetached by a (pulsed) excimer-pumped dye laser. The dyes used for photodetachment of Si_4^- were Coumarin 503 (479–553 nm), Exalite 416 (402–427 nm), DPS (399–415 nm), BBQ (367–405 nm), QUI (368–402 nm), DMQ (346–377 nm), pTp (332–350), and, doubled with a β-barium borate (BBO) crystal, Rhodamine 640 (310–332 nm), and Rhodamine 590 (287–300 nm).

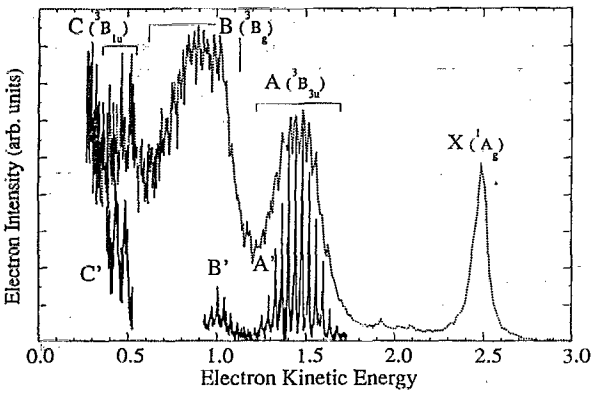

FIG. 3. The ZEKE spectrum of Si_4^- (solid lines) is superimposed onto the energy scale of the PES of Si_4^- obtained using 4.66 eV photon energy (dotted line).

Threshold photodetachment spectra are obtained by adapting the ZEKE spectroscopy method developed by Müller-Dethlefs *et al.*[20] to negative ion photodetachment. In this experiment, the Si_4^- is photodetached in the region marked by the $\times$ on Fig. 2. The photoelectrons are extracted with a delayed, pulsed field. This allows the higher energy photoelectrons to spatially separate from the threshold electrons, which have nearly zero kinetic energy. The energetic electrons that scatter away from the ion beam axis are discriminated against by apertures located in the detector region. Those that scatter along the ion beam arrive at the detector at different times from the threshold electrons and are discriminated against by gated integration of the threshold electrons. This combination of spatial and temporal discrimination yields an electron energy resolution of 3 cm^{-1}.

As an alternative mode of operation, the photoelectrons can be extracted immediatedly upon photodetachment. This results in spectral features that are 150 cm^{-1} wide but have considerably higher intensity. While no high resolution information can be obtained in this mode of operation, it is useful as a first order method of locating the *s*-wave photodetachment thresholds, especially when the photodetachment signal is too small to obtain ZEKE spectra.

Total photodetachment cross section scans were also performed for Si_4^- to determine whether any high-lying (autodetaching or bound) excited anion states existed for Si_4^- as they did for C_6^-.[26] No such states were found, and this experiment will not be discussed further.

III. RESULTS

The spectrum of Si_4^- obtained on the threshold photodetachment apparatus is shown superimposed on the photoelectron spectrum of Si_4^-[17] in Fig. 3. In the ZEKE mode of operation, we saw the two bands labeled A' and B'. Band A' corresponds well with band A seen in the PES, but band B' falls primarily on the rising edge of band B in the PES. No structure is seen in the ZEKE spectrum for the remainder of the energy range spanned by the PES band B. Band C', which corresponds to band C in the PES, could

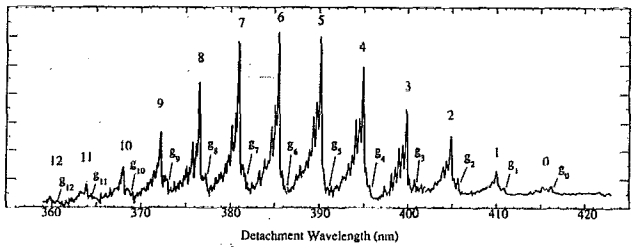

FIG. 4. Expanded-scale, finer-step scan of the A' band.

only be observed in the partially discriminated mode of operation due to its low signal intensity; this is why the features in this band are broader. No signal corresponding to band X (the transition to the Si_4 ground state) in the PES could be observed in either the ZEKE or partially discriminated mode. Hence, the three observed bands all involve transitions to excited states of Si_4. The bands will now be examined in greater detail.

A. Band A'

Band A' in the threshold photodetachment spectrum shows a progression of up to 14 peaks which corresponds to the partially resolved vibrational structure seen previously in the Si_4^- PES.[17] The PES had to be shifted along the abscissa by -0.03 eV in order to fully align the PES and ZEKE progressions. Assuming this shift applies to the entire photoelectron spectrum, the electron affinity of Si_4 previously obtained from the PES should be changed slightly to 2.17 ± 0.01 eV. Figure 4 shows a finer step, signal averaged scan of this band. Clearly, each member of this progression consists of groups of smaller peaks found to either side of a single, more intense peak. The intense peak in each group is labeled by number and the positions and spacings of these peaks are listed in Table I. The average peak spacing is 312 cm^{-1}.

Figure 5 shows a more expanded scale scan of the two groups of peaks around peaks 3 and 4. The more intense side peaks, labeled a_n through e_n, shade to higher photon energy relative to the most intense peak (peak n) in each group, while the less intense side peaks, labeled f_n and g_n, shade to lower photon energy. The positions and energies of these side progressions are listed in Table II for the two groups shown in Fig. 4. All of the main and side peaks are between 16 and 20 cm^{-1} wide (FWHM). We note that this pattern of peaks occurs, with some intensity variation, for every group of peaks in band A'.

The intensities of peaks a_n through g_n are dependent on source conditions. When we produced ions using a solenoid-type pulsed molecular beam valve (i.e., higher temperature) instead of the piezoelectric valve, a_n and b_n were as intense as the main peak n while c_n through e_n remained unresolved in a broad signal with half the intensity of the n–a_n–b_n triplet. The intensities of peaks g_n and f_n are also dependent on source conditions, although they never exceeded one half the n peak intensity. This source condition dependence indicates that these peaks are due to transitions from vibrationally excited levels of the anion,

TABLE I. Positions, spacings and tentative assignments for the main peaks in the A' band of Si_4^-.

Peak	Position (nm)	Spacing (cm^{-1})[a]	Tentative assignment[b]
0	415.27(14)		Origin
		314	
1	409.93(13)		2_0^1
		311	
2	404.77(13)		2_0^2
		308	
3	399.78(13)		2_0^3
		313	
4	394.84(12)		2_0^4
		310	
5	390.06(12)		2_0^5
		311	
6	385.39(12)		2_0^6
		308	
7	380.87(12)		2_0^7
		308	
8	376.46(11)		2_0^8
		308	
9	372.15(11)		2_0^9
		305	
10	367.98(11)		2_0^{10}
		310	
11	363.83(11)		2_0^{11}
		306	
12	359.83(10)		2_0^{12}
		303	
13	355.95(10)		2_0^{13}

[a]Error for each spacing is ± 11 cm^{-1}.
[b]Based on peak 0 being the origin.

or, "hot-band" transitions. The assignments of these peaks are addressed in the following section.

At first glance, peaks a_n through e_n appear to belong to one progression with a spacing of ~ 25 cm^{-1}. However, the intensity distribution of these peaks indicate otherwise. Peak b_n is typically of comparable intensity to a_n, whereas peak c_n is quite small compared to b_n, if it can be resolved at all. Therefore, peaks a_n through e_n appear to involve two vibrational modes. For instance, b_n has an average spacing from n of 53 cm^{-1}, and d_n is 51 cm^{-1} from b_n on average, and for several of the main spectral features, an e_n peak can also be seen approximately 50 cm^{-1} to the blue of peak d_n.

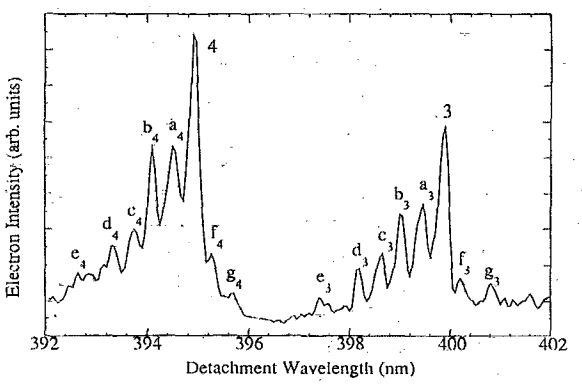

FIG. 5. Expanded-scale, finer-step scan of peaks 3 and 4 of the A' band.

TABLE II. Positions, relative spacings, and tentative assignment of sequence bands found around peaks 3 and 4 in the A' band of Si_4^-.

Peak	Position (nm)	Spacing from main feature (cm^{-1})[a]	Tentative assignment
g_3	400.74(13)	−59	2_1^4
f_3	400.13(13)	−21	$2_0^3 3_1^1$
3	**399.78(13)**	**0**	2_0^3
a_3	399.40(13)	24	$2_0^3 6_1^1$
b_3	398.94(13)	53	$2_0^3 5_1^1$
c_3	308.56(13)	74	$2_0^3 5_1^1 6_1^1$
d_3	398.09(13)	107	$2_0^3 5_2^2$
e_3	397.34(13)	154	$2_0^3 5_3^3$
g_4	395.56(12)	−46	2_1^5
f_4	395.19(12)	−22	$2_0^4 3_1^1$
4	**394.84(12)**	**0**	2_0^4
a_4	394.39(12)	29	$2_0^4 6_1^1$
b_4	393.99(12)	55	$2_0^4 5_1^1$
c_4	393.64(12)	77	$2_0^4 5_1^1 6_1^1$
d_4	393.29(12)	100	$2_0^4 5_2^2$

[a]Error for each spacing is ± 11 cm^{-1}.

The a_n peaks are spaced approximately 30 cm^{-1} from peak n for low n, but this spacing decreases down to 26 cm^{-1} to higher values of n. The same effect is seen for the energy difference between c_n and b_n in those cases where c_n is well enough resolved. Therefore, we believe that n, b_n, d_n, and e_n belong to a 50 cm^{-1} progression in one mode, and that n, a_n, and b_n, c_n represent shorter 30 cm^{-1} progressions in a second mode.

The side peaks found to the red of the main peak are fewer and less intense. The f_n peaks are found approximately 25 ± 5 cm^{-1} to the red of peak n. In some cases, such as for $n=5$, f_n appears to be hardly resolved from the main peak. The g_n peaks are found approximately 53 ± 5 cm^{-1} to the red of the main peaks n. Figure 4 shows that the intensities of the g_n peaks relative to the main peaks is not constant throughout the progression; for $n=0$–3, the g_n peaks are fairly prominent, but peaks g_5 and g_6 cannot be discerned from the noise. For $n>8$, the g_n peaks again become apparent.

B. Band B'

As can be seen from the ZEKE portion of the spectrum shown in Fig. 3, band B' is much less intense than band A'. In addition, the progression is much shorter. Note that while band A' closely matches band A in the photoelectron spectrum, band B' covers a much smaller energy range than band B in the PES. No structure was seen between band B' and 300 nm, even using the partially discriminated cross section mode of the apparatus. Figure 6 shows band B' on an expanded scale. Because the signal was so much less for this band, the signal-to-noise ratio is not as good as for band A'.

Again, the members of the progression in this band appear as groups of peaks, but the profiles and relative intensities of groups exhibit irregularity. The first three members of the progression are qualitatively similar in profile to those found in the band A' in that the groups are

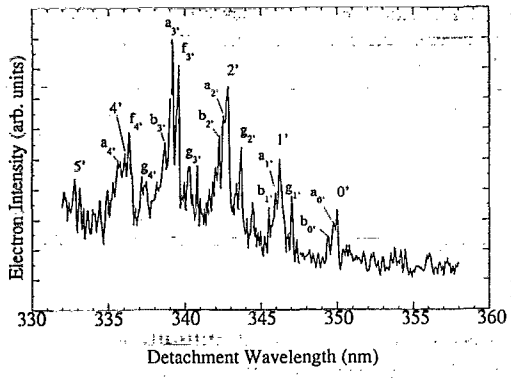

FIG. 6. Expanded-scale scan of the B' band.

dominated by a central intense peak, labeled n', as well as fairly intense side peaks, $a_{n'}$ and $b_{n'}$, found to higher photon energy and a less intense side peak, $g_{n'}$, at lower photon energy. The central peaks n' in the first three groups seem to form a short, 300 ± 6 cm^{-1} progression. However, the profiles of the fourth and fifth groups are quite different. There is no peak at the correct position in the fourth group to be a part of the 300 cm^{-1} progression, although the average position of the two intense peaks labeled $a_{3'}$ and $f_{3'}$ is just where peak 3′ would be expected. In the fifth group, peak 4′, while apparently part of the main 300 cm^{-1} progression, is noticeably less intense than the peaks to either side. Peak 5′ can barely be discerned from the noise. Peak positions and spacings for band B' can be found in Table III.

TABLE III. Positions and relative spacings of the peaks found in the B' band of Si_4^-.

Peak	Position (nm)	Relative spacing (cm^{-1})[a]
0′	**349.90(12)**	**0**
$a_{0'}$	349.70(12)	16
$b_{0'}$	349.35(12)	45
$g_{1'}$	347.0(12)	239
1′	**346.20(12)**	**305**
$a_{1'}$	345.86(12)	334
$b_{1'}$	345.40(14)	372
$g_{2'}$	343.61(12)	529
2′	**342.69(12)**	**602**
$a_{2'}$	342.41(12)	625
$b_{2'}$	342.13(14)	649
$g_{3'}$	340.22(12)	814
$f_{3'}$	339.45(8)	880
$a_{3'}$	339.00(8)	918
$b_{3'}$	338.60(11)	954
$g_{4'}$	337.21(17)	1076
$f_{4'}$	336.26(11)	1160
4′?	**336.96(11)**	**1186**
$a_{4'}$	335.61(15)	1217
5′	**332.71(11)**	**1477**

[a]Error for spacing is ± 14 cm^{-1}.

C. Band C'

We were restricted to examining this band using the partially discriminated cross section mode of the apparatus due to very low photoelectron signal. The low signal is due to small photodetachment cross section near threshold for this state and lower photodetachment laser power.

The broad features of band C' shown in Fig. 3 are roughly 200 cm^{-1} wide and are separated by approximately 430 cm^{-1} peak to peak. The broad peaks are not perfectly symmetric; there are probably many sequence bands (as were seen for the higher resolution sections of the spectrum) and/or combination features contributing to the profile of these features.

IV. ANALYSIS AND DISCUSSION

According to Rohlfing and Raghavachari,[4] the $^2B_{2g}$ anion ground state has the valence orbital configuration $\cdots(b_{3g})^2(b_{3u})^2(a_g)^2(b_{1u})^2(b_{2g})^1$. Electrons removed from either the b_{1u} or the b_{3u} orbitals can depart via s-wave photodetachment, while this is not the case for the b_{2g} or a_g orbitals.[22] Therefore, according the assignment of the Si_4^- PES in Ref. 4, (see band labels on Fig. 1)[4] we would expect to see bands A and C in the ZEKE spectrum, which we do, since these states result from the removal of an electron from the b_{1u} and b_{3u} orbitals, respectively. Band X in the PES is *not* seen in the ZEKE spectrum, which is consistent with its assignment to the $^1A_g + e^- \leftarrow {}^2B_{2g}$ transition. This transition involves removing the b_{2g} electron, which would depart as a p wave. Band B seen in the PES was assigned[4] to the $^3B_g + e^- \leftarrow {}^2B_{2g}$ transition, corresponding to removal of an a_g electron. This transition, therefore, should *not* be apparent in the ZEKE spectrum, but we do observe band B' which corresponds to the rising edge of band B in the PES. As discussed below, we believe band B is due to overlapping electronic transitions, one of which can occur by s-wave detachment. We now consider all three bands in the ZEKE spectrum in more detail.

A. Band A'

The energy of band A' and the fact that we observe it in the ZEKE spectrum is consistent with the *ab initio* assignment of this band to the $^3B_{3u} + e^- \leftarrow {}^2B_{2g}$ transition.[4] The progression of the central peaks (peaks n in Fig. 4) can be fit with the harmonic frequency $\omega_e = 312 \pm 1$ cm^{-1} and a very small anharmonic constant $\omega_e x_e = 0.3 \pm 0.1$ cm^{-1}. The harmonic frequency is very close to the *ab initio* value of 306 cm^{-1} for the $\nu_2(a_g)$ mode in the Si_4 $^3B_{3u}$ state. Moreover, the *ab initio* geometries for Si_4^- and the $^3B_{3u}$ state of Si_4, which are shown in Fig. 7 along with the ν_2 and ν_1 (a_g) normal modes of the $^3B_{3u}$ neutral (the force constants for determining the normal modes were obtained from our own *ab initio* calculations on Si_4) suggest a large displacement along the ν_2 normal coordinate upon photodetachment, but almost no displacement along the higher frequency ν_1 normal coordinate. Hence, the ν_2 mode should be the only active vibration in the ZEKE spectrum. We therefore assign peaks n to the 2_0^n progression.

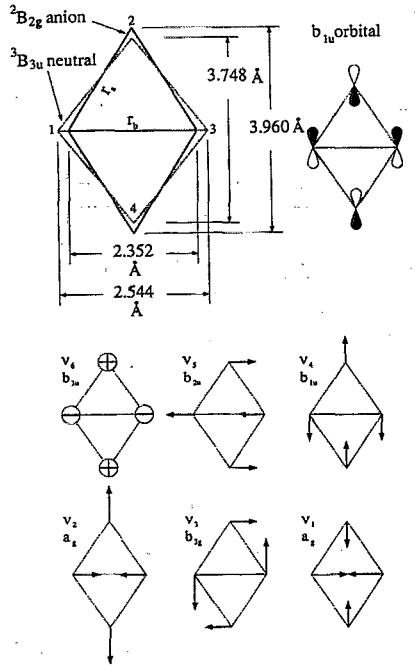

FIG. 7. Calculated geometries of the ground $^2B_{2g}$ anion state and the neutral $^3B_{3u}$ state (Ref. 4), the orbital from which an electron is removed in the transition between the two states, and the normal coordinates of the $^3B_{3u}$ state of Si_4.

Although the assignment of the 2_0^n progression is straightforward, locating the origin is somewhat more ambiguous. Peak 0, located at 415.27 nm, appears to be the lowest energy peak in the 312 cm^{-1} progression, but one could argue that there is a small peak buried under noise at 312 cm^{-1} lower in energy (420.68 nm), or even 624 cm^{-1} to the red of peak 0 (426.28 nm) where no detectable electron signal was seen.

We attempted to determine the location of the origin and the actual normal mode displacement by performing a single mode (ν_2) Franck–Condon simulation of the spectrum. Simulations performed assuming the origin was at 415.27 nm [with ΔQ of 0.219±0.008 Å(amu)$^{1/2}$], 420.68 nm [$\Delta Q \sim 0.235 \pm 0.008$ Å(amu)$^{1/2}$], or 426.28 nm [ΔQ 0.259±0.008 Å(amu)$^{1/2}$] all satisfactorily matched the experimental progression. However, based on the *ab initio* geometries and force constants, we can calculate the ν_2 normal mode displacement between the anion and neutral. We find this to be 0.208 Å(amu)$^{1/2}$, which is in best agreement with the normal coordinate displacement assumed for the simulation with the origin at 415.27 nm. We therefore take this to be the origin. The excitation energy of the $^3B_{3u}$ state is then 0.815 ± 0.010 eV (listed in Table IV) which is in good agreement with the 0.85 eV excitation energy calculated by Rohlfing and Raghavachari.[4]

We next consider the set of peaks g_n, each of which is located 53 cm^{-1} to the red of the corresponding central peak n. The bimodal intensity distribution of these peaks, passing through a minimum at $n=5$–6, can be explained by assigning them to a hot-band progression in the the ν_2 mode originating from the $\upsilon_2=1$ level of the anion, i.e., a

TABLE IV. Excitation energies for several of the low-lying states of Si_4.

State of Si_4	T_e (eV)
$^3B_{1u}$	2.01 ±0.02
$^1B_{3u}$	1.37 ±0.01
$^3B_{3u}$	0.815±0.010
^1A_g	0
	(E.A.=2.17±0.01)

2_1^n progression. The intensity minimum can be qualitatively understood by referring to Fig. 8, which shows anion and neutral harmonic potential energy curves displaced along the Q_2 coordinate by 0.219 Å(amu)$^{1/2}$, the displacement that best reproduced the intensity distribution of the main progression (peaks n). This displacement is such that a node in the neutral $\upsilon_2=6$ wave function coincides with one of the the maxima of the anion $\upsilon_2=1$ wave function, causing the overlap to be close to zero. Based on this assignment, the ν_2 frequency in the anion is 365 cm^{-1}, quite close to the *ab initio* frequency[4] of 383 cm^{-1}. The intensity distribution of peaks n and g_n can be satisfactorily reproduced in a one-dimensional simulation (not shown) where the vibrational temperature of the anions is assumed to be 200 K.

The large geometry change and fairly large frequency change in the ν_2 mode between the anion and neutral can be explained by considering the orbital from which the electron is removed in the neutral←anion transition. The b_{1u} orbital is formed by the (in-plane) p_z orbitals (see Fig. 7) which effectively bonds the silicon atoms labeled 1 and 3. Removal of an electron from this orbital will weaken this bond, resulting in the longer bond distance and lower ν_2 frequency in the neutral, since this mode primarily involves the stretching of r_b.

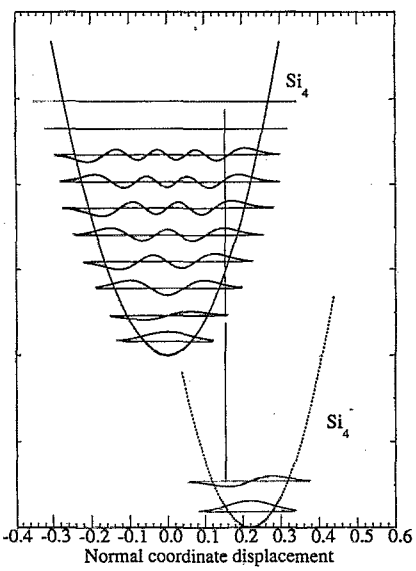

FIG. 8. One-dimensional potential energy curves for the anion and neutral ν_2 modes. The anion potential is displaced by the amount determined in the simulation of band A'.

We next consider the other vibrational features in band A', peaks a_n–f_n. As mentioned earlier, these peaks originate from vibrationally excited levels in the anion, and we assign them to sequence bands in modes other than the ν_2 mode, that is, $2_0^n m_1^1$, $2_0^n m_2^2$, etc., transitions. There are five other normal modes of Si_4/Si_4^- that could be contributing to this structure. However, using a vibrational temperature of 200 K as a guideline, significant population is expected only in the four lowest frequency modes of the anion. In order of increasing frequency, these are calculated[4] to be the ν_6 (165 cm^{-1}), ν_5 (295 cm^{-1}), ν_2 (383 cm^{-1}), and ν_3 (390 cm^{-1}) modes. The normal modes are shown in Fig. 7.

The ν_2 mode has already been accounted for. The f_n peaks, each of which lies 25 cm^{-1} to the blue of the main peak n, are of comparable intensity to the most intense g_n peaks, and likely originate from the $v=1$ level of a mode close in frequency to the ν_2 mode. According to the *ab initio* results, the most likely candidate is the ν_3 mode, and we therefore assign peaks f_n to the $2_0^n 3_1^1$ progression. Although we cannot directly extract the ν_3 anion and neutral frequencies from the peak positions, they do yield the *difference* between the anion and neutral frequencies, and show that the ν_3 mode is 25 cm^{-1} lower in the neutral. This is consistent with the *ab initio* results, which give $\nu_3=367$ cm^{-1} in the neutral, 23 cm^{-1} less than the calculated anion frequency. As discussed earlier, peaks a_n–e_n to the red of peak n appear to be sequence bands composed of two overlapping progressions. The presence of sequence bands to the red of the central peak means that the vibrational modes involved have higher frequencies in the neutral than in the anion. This is at odds with the *ab initio* results,[4] for which *all* of the frequencies for the Si_4 $^3B_{3u}$ state are lower than in the anion. Since the leading members of these progressions, peaks a_n and b_n, are quite intense, these progressions most likely involve the two lowest frequencies of the anion, the ν_5 and ν_6 modes. From the positions of peaks a_n and b_n relative to peak n, the frequencies of one of these modes is 27 cm^{-1} higher in the neutral than in the anion, while the other is 52 cm^{-1} higher in the neutral. In contrast, the *ab initio* calculations predict the ν_5 and ν_6 frequencies to be higher in the anion by 118 and 8 cm^{-1}, respectively.

We therefore have two possible assignments for these peaks. In one assignment, peak a_n is the $2_0^n 6_1^1$ transition and peak b_n is primarily the $2_0^n 5_1^1$ transition (with some contribution from the $2_0^n 6_2^2$ transition). These assignments and those of peaks c_n–e_n are listed in Table II. In the other assignment, ν_5 and ν_6 are switched. In order to better choose between these assignments, we can simulate the spectrum using the four modes considered above (ν_2, ν_3, ν_5, ν_6). We do this first for the assignment in Table II. For the ν_5 and ν_6 modes, we need to assume values for the neutral frequencies, and these will fix the anion frequencies. If we choose the *ab initio* values for the neutral frequencies, the anion frequencies are those given in Table V. We obtain the simulation shown in Fig. 9 using 200 K as the vibrational temperature for the ν_2 mode and slightly different vibrational temperatures for the other three modes (listed in Table V). The temperatures were fit paying closest attention to peak groups with $n=3$ and 4, since our data is best for these (see inset, Fig. 9).

TABLE V. Si_4 neutral and anion frequencies along with anion vibrational temperature assumed for the spectral simulation shown in Fig. 7. The alternative interpretation of the spectrum for ν_5 and ν_6 is shown in parenthesis. Also included are calculated anion frequencies.

Mode	Neutral frequency (cm^{-1})	Anion frequency (cm^{-1})	Temperature (K)	Calc.[b] anion freq. (cm^{-1})
ν_2	312[a]	365	200	383
ν_3	367	392	270	390
ν_5	177	125(150)	170(380)	295
ν_6	159	132(107)	290(120)	165

[a]Calculated neutral frequency for ν_2 is 306 cm^{-1}.
[b]Reference 4.

The reasonable fit between the simulated and experimental spectrum using vibrational temperatures close to 200 K for all four modes offers indirect support both for the assignment of peaks a_n–e_n and for using the *ab initio* frequencies for the neutral. While different modes have different cooling efficiencies in a free jet expansion, we would expect the temperatures of the remaining modes to be in the neighborhood of 200 K, the appropriate temperature for the ν_2 mode, particularly if they have similar or lower frequencies. If we use the alternate assignment proposed above, with the ν_5 and ν_6 modes switched from Table II, and use the *ab initio* values for the neutral frequencies, then the anion frequencies are $\nu_5=150$ cm^{-1} and $\nu_6=107$ cm^{-1}, and the required vibrational temperatures are 380 and 107 K, respectively (these values are included parenthetically in Table V). This is a noticeably larger deviation from 200 K than the values obtained using the former assignment, and makes this assignment somewhat less desirable.

Another option is to use the *ab initio* ν_5 and ν_6 frequencies for the anion (see Table V), and fix the neutral

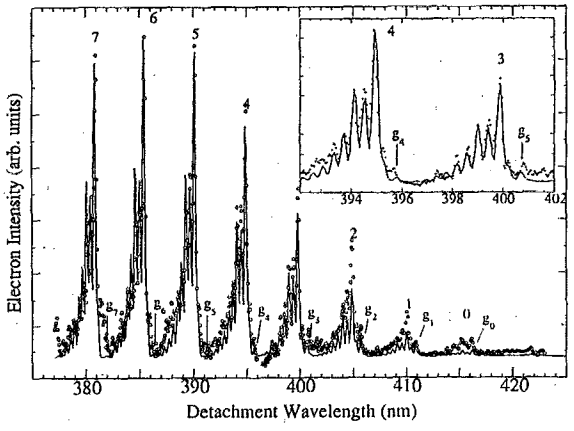

FIG. 9. Four mode Franck–Condon simulation (solid line) of the A' band (circles). The inset shows an expanded scale view of the simulation. Those peaks labeled explicitly by n or g_n are due to excitations in the ν_2 mode of the anion and/or neutral.

frequencies accordingly. Using the peak assignments in Table II, we require vibrational temperatures of 650 and 450 K for the ν_5 and ν_6 modes, respectively. These temperatures for the lowest frequency modes seem unreasonably large compared to the 200 K temperature for the ν_2 mode. A similiarly large deviation is obtained using the alternate assignment assuming the *ab initio* anion frequencies.

Overall, the peak assignments in Table II and the frequencies listed in Table V seem the most reasonable of all the possibilities considered. The small frequency change in the ν_6 mode upon photodetachment to the $^3B_{3u}$ state is sensible as it is an out-of-plane vibration whereas the b_{1u} orbital is primarily in the plane of the molecule. The increase in the ν_5 frequency upon photodetachment is more difficult to rationalize on the basis of molecular orbital considerations.

The spectra support the *ab initio* geometries for Si_4^- and the Si_4 excited state, as well as the *ab initio* frequencies for the anion and neutral ν_2 and ν_3 modes. However, the spectra are inconsistent with the *ab initio* ν_5 and ν_6 frequencies. The ν_5 frequency for the anion is particularly suspect, since it lies well above the predicted neutral frequency, whereas our spectrum shows it should be less than the neutral frequency. Moreover, a high vibrational temperature for the ν_5 mode is always needed to simulate the spectrum if the *ab initio* value is used. It is possible that the the large discrepancy between the *ab initio* Si_4/Si_4^- ν_5 frequency difference and the observed frequency difference is due to an incorrect assignment of the b_n peaks. For instance, b_n could be due to a combination band; if b_n were due to the $2_0^{n-1}5_0^2$ transition, its position would be in fairly good agreement with the calculated ν_5 frequency. However, were this the case, peak b_0 (found 50 cm^{-1} from the origin) would not appear in the spectrum. Also, the intensity of the b_n peaks is too high for a $\Delta v=2$ transition in a nontotally symmetric mode. Thus we believe our assignment of the b_n peaks to sequence band transitions is correct. In any case, independent measurements of either the anion or neutral ν_5 and ν_6 frequencies would result in a more complete understanding of the ZEKE spectrum.

B. Band *B'*

Rohlfing and Raghavachari assigned band B shown on the PES (Fig. 1) to the $^3B_g+e^- \leftarrow {}^2B_{2g}$ transition,[4] where the ^3B_g state has a C_{2h} structure resulting from a slight distortion of the $^3B_{2g}$ (D_{2h}) state. They pointed out that the irregular spacings of the band may be due to contributions from the nearby $^3B_{1g}$, $^1B_{2g}$, and $^1B_{3u}$ states. However, only the $^1B_{3u}$ state is accessible from the anion by s-wave detachment. This suggests that band B' in the ZEKE spectrum and the leading edge of band B in the photoelectron spectrum are due to the $^1B_{3u}+e^- \leftarrow {}^2B_{2g}$ transition. The $^1B_{3u}$ state is the singlet counterpart of the $^3B_{3u}$ state responsible for band A', so the apparent origin of band B' at 349.90 nm implies a singlet–triplet splitting of 0.558 eV for the B_{3u} state. This is lower than the calculated splitting, 1.04 eV, but the disagreement is not so unreasonable considering the degree of difficulty in accurately calculating singlet–triplet splittings in complex molecules.

The profile of band B' is very different from band A', with the intensity of band B' falling off after only a few peaks. Moreover, the vibrational structure in band B' is irregular. As mentioned in Sec. III, the first three groups of peaks in this band (Fig. 5) are similar to the peak groups in the band A'. The spacing of the central peaks 0′–2′ is 300(8) cm^{-1}, and the fairly intense sequence bands occurring to the red of these features ($g_{n'}$) are spaced such that the anion frequency is approximately 365 ± 5 cm^{-1}. Thus the n' peaks appear to be a progression in the ν_2 mode of the neutral $^1B_{1u}$ state, with a frequency 12 cm^{-1} lower than the ν_2 mode in the $^3B_{1u}$ state. The fourth group of peaks is very different; it is an intense doublet separated by approximately 38 cm^{-1}. These peaks, $f_{3'}$ and $a_{3'}$ are separated by 279 and 317 cm^{-1} from the peak 2′, so it seems that the 300 cm^{-1} progression stops at peak 2′. It is true that the signal-to-noise ratio of this band is not very good and the spacings between either $f_{3'}$ or $a_{3'}$ and peak 2′ fall almost within the experimental uncertainty of the 300 cm^{-1} progression. However, the $a_{3'}$ and $f_{3'}$ peaks are well resolved from each other, while the peaks 2′, 1′, and 0′ are poorly resolved from the adjacent transitions. Thus the pattern of transitions in the fourth group is clearly different from the lower energy groups of peaks.

Since the band B' does not span the energetic extent of band B in the PES, there must be at least one dark state lying close to the $^1B_{3u}$ state. By this, we mean a Si_4 electronic state which is not accessible by s-wave detachment and therefore is seen in the PES but not the ZEKE spectrum; this includes all three of the other electronic states predicted to occur in the vicinity of band B. Hence, a possible explanation for the vibrational irregularity of band B' is that the higher vibrational levels of the $^1B_{3u}$ state are vibronically coupled to one of these dark states.

As examples of possible vibronic coupling schemes, any totally symmetric vibrational level of the $^1B_{3u}$ state could be coupled with odd vibrational levels in a b_{1u} mode of the $^1B_{2g}$ state, odd b_{2u} levels of the $^3B_{1g}$ state, or odd b_u levels of the ^3B_g state. Given that the three candidate states for vibronic coupling are all predicted to lie within 0.3 eV of where we observe the $^1B_{3u}$ state, one might expect the dominant coupling to be with the $^1B_{2g}$ state, as this is the only nearby state with the same spin multiplicity.

The peak pattern for the fourth group is what one might expect under the following circumstances. Suppose a v_4=odd level (b_{1u} vibrational symmetry—see Fig. 7) of the $^1B_{2g}$ state were accidentally degenerate with the $v_2=3$ level of the $^1B_{3u}$ state, at the energy where peak 3′ would normally occur. The two vibronically coupled levels will mix and repel one another, and a 38 cm^{-1} splitting via this interaction would yield peaks $a_{3'}$ and $f_{3'}$. Peak $a_{3'}$ then consists of two overlapped transitions-one due to the higher energy transition resulting from the vibronic coupling interaction, and the other from the transition analogous to peaks $a_{0'}$–$a_{2'}$ (see below). Clearly, such a mechanism must be regarded as speculative, but it is certainly not unreasonable given the large number of nearby electronic states.

The 4′ group is most likely affected in a similar man-

ner, but due to the poor S/N, it is difficult to get a precise idea of what could be happening with it. The chance of vibronic coupling only increases at higher energies due to presence of more combination bands with the appropriate vibronic character, so we would only expect it to be increasingly difficult to analyze these higher energy peaks.

There remain several other issues regarding this band. It has been mentioned that the profiles of the first three groups of peaks in the B' band are qualitatively similar to those in the A' band, but not exactly. For example, the spacing between peaks $a_{n'}$ and n' in band B' is slightly smaller than between peaks a_n and n in band A'. If the $a_{n'}$ peaks are due to sequence bands in the ν_6 mode, a difference between the neutral singlet and triplet ν_6 frequencies of about 5 to 10 cm^{-1} (the triplet frequency being higher) would account for this. Also, the origin of this band has not been definitively identified, although we assign it to peak 0′, the central peak of the lowest energy group identified with band B'. However, the lower signal to noise associated with band B' may cause the actual origin to be obscured. The excitation energy of the $^1B_{3u}$ state assuming peak 0′ to be the origin is 1.37 ± 0.010 eV (see Table IV). While we cannot determine the origins of the $^1B_{2g}$, ^3B_g, or $^3B_{1g}$ states, our vibronic coupling hypothesis requires at least one of them to lie quite close to the $^1B_{3u}$ state.

C. Band C'

While not much information can be extracted from the broad features comprising band C', a few words on its assignment are warranted. This band, which was assigned to the $^3B_{1u}+e^- \leftarrow {}^2B_{2g}$ transition,[4] lies approximately 1.2 eV above band A'. This raises the possibility that band C' is due to the transition to the $^1B_{3u}$ state (the singlet–triplet splitting for B_{3u} was calculated to be 1.04 eV) and that band B' is the $^3B_{1u}+e^- \leftarrow {}^2B_{2g}$ transition. However, this possibility is unlikely for the following reason. From the *ab initio* geometries, the ν_1 mode should be active in transitions to the $^3B_{1u}$ state. The ν_1 frequencies of all of the excited D_{2h} Si_4 states are around 400 cm^{-1} or greater. The B' progression is approximately 300 cm^{-1}, while the peak spacing in band C' is roughly 430 cm^{-1}, consistent with a ν_1 progression. We therefore believe that the assignment of band C' made by Rohlfing and Raghavachari is correct.[4]

V. CONCLUSION

The results presented here represent a far more detailed experimental probe of the vibrational and electronic structure of silicon tetramer than our previous photoelectron spectroscopy study. We have obtained several vibrational frequencies for the anion and various electronic states of the neutral, particularly the $^3B_{3u}$ excited state, as well as excitation energies for several electronic states.

Our results also emphasize the interaction between theory and experiment in understanding the spectroscopy of clusters. The role of *ab initio* calculations in interpreting these spectra cannot be overemphasized. In the absence of experimental force constants for Si_4, *ab initio* calculations are needed to perform any reasonable assignment of the observed vibrational progressions. Moreover, given the complex electronic structure of a species such as Si_4, the assignment of electronic bands to specific neutral←anion transitions also requires some *ab initio* input.

Our experimental results provide a detailed comparison with the calculations. We find from band A' that the excitation energy for the Si_4 $^3B_{3u}$ state is in excellent agreement, as are the vibrational frequencies for the ν_2 mode in the anion and this state of the neutral. The sequence band structure in band A' is consistent with the *ab initio* values for the ν_3 mode in the anion and neutral, but not with the *ab initio* values for the ν_5 and ν_6 modes. Our results also show that band B in the Si_4^- photoelectron spectrum is due to transitions to overlapping electronic states, as suggested in the calculations, but the ZEKE spectrum implies that the lowest energy of these is the Si_4 $^1Si_{3u}$ state, whereas the calculations predict this to be about 0.5 eV higher than where we observe it. Finally, on the basis of the observed vibrational progression, we find the *ab initio* assignment of band C to the transition to the Si_4 $^3B_{1u}$ state to be reasonable.

We feel that these comparisons between experiment and theory will become even more essential as we begin to study the larger Si clusters via threshold photodetachment spectroscopy. Many of these are predicted to exhibit several low-lying structures with very different geometries. A comparison of experimental and theoretical vibrational frequencies and electronic excitation energies will facilitate sorting out these possible cluster structures.

ACKNOWLEDGMENTS

This research is supported by the National Science Foundation under Grant No. DMR-9201159. We thank C. M. Rohlfing for several stimulating discussions.

[1] For example, see P. W. Merrill, Publ. Astron. Soc. Pac. **38**, 175 (1926); R. F. Sanford, Astrophys. J. **111**, 262 (1950); B. Kleman, Astrophys. J. **123**, 162 (1950), and references therein.

[2] P. Ho and W. G. Breiland, App. Phys. Lett. **44**, 51 (1984).

[3] K. Raghavachari and C. M. Rohlfing, J. Chem. Phys. **94**, 3670 (1991); C. M. Rohlfing and K. Raghavachari, Chem. Phys. Lett. **167**, 559 (1990); K. Raghavachari, Z. Phys. D **12**, 61 (1989); K. Raghavachari, J. Chem. Phys. **84**, 5672 (1986); K. Raghavachari and V. Logovinsky, Phys. Rev. Lett. **55**, 26 (1985); K. Raghavachari, J. Chem. Phys. **83**, 3520 (1985).

[4] C. M. Rohlfing and K. Raghavachari, J. Chem. Phys. **96**, 2114 (1992).

[5] R. Fournier, S. B. Sinnott, and A. DePristo, J. Chem. Phys. **97**, 4149 (1992); S. D. Li, R. L. Johnston, and J. N. Murrell, J. Chem. Soc. Faraday Trans. **88**, 1229 (1992); D. G. Dai and K. Balasubramanian, J. Chem. Phys. **96**, 3279 (1992); L. Adamowicz, Chem. Phys. Lett. **188**, 131 (1992); **185**, 244 (1991); S. Katircioglu and S. Erkoc, *ibid.* **184**, 118 (1991); K. Balasubramanian, *ibid.* **135**, 283 (1987); **125**, 400 (1986); G. Pacchioni and J. Koutecky, J. Chem. Phys. **84**, 3301 (1986); J. R. Sabin, J. Oddershede, G. H. F. Diercksen, and N. E. Gruner, *ibid.* **84**, 354 (1986); Z. Slanina, Chem. Phys. Lett. **131**, 420 (1986); R. S. Grev and H. F. Schaefer, *ibid.* **119**, 111 (1985); R. O. Jones, Phys. Rev. A **32**, 2589 (1985).

[6] A. E. Douglas, Can. J. Phys. **33**, 801 (1955); R. D. Verma and P. A. Warsop, *ibid.* **41**, 152 (1963); I. Dubois and H. Leclerq, *ibid.* **49**, 3053 (1971); S. P. Davis and J. W. Brault, J. Opt. Soc. Am. B **4**, 20 (1987).

[7] For example, see J. R. Heath, Y. Liu, S. C. O'Brien, Q.-L. Zhang, R. F. Curl, K. Tittel, and R. E. Smalley, J. Chem. Phys. **83**, 5520 (1985); Y. Liu, Q.-L. Zhang, F. K. Tittel, R. F. Curl, and R. E. Smalley, *ibid.* **85**, 7434 (1986); L. A. Bloomfield, R. R. Freeman, and W. L. Brown, Phys. Rev. Lett. **54**, 2246 (1985).

[8] J. R. Heath, Y. Liu, S. C. O'Brien, Q.-L. Zhang, R. F. Curl, F. K. Tittel, and R. E. Smalley, J. Chem. Phys. **83**, 5520 (1985).
[9] M. L. Mandich, V. E. Bondybey, and W. D. Reents, Jr., J. Chem. Phys. **86**, 4245 (1987).
[10] W. Weltner, Jr. and D. McLeod, Jr., J. Chem. Phys. **41**, 235 (1964).
[11] T. P. Martin and H. Schaber, Z. Phys. B **35**, 61 (1979).
[12] C. B. Winstead, K. X. He, T. Hammond, and J. L. Gole, Chem. Phys. Lett. **181**, 222 (1991).
[13] C. Jin, K. J. Taylor, J. Conceicao, and R. E. Smalley, Chem. Phys. Lett. **175**, 17 (1990).
[14] O. Cheshnovsky, S. H. Yang, C. L. Pettiette, M. J. Craycraft, Y. Liu, and R. E. Smalley, Chem. Phys. Lett. **138**, 119 (1987).
[15] M. R. Nimlos, L. B. Harding, and G. B. Ellison, J. Chem. Phys. **87**, 5116 (1987).
[16] T. N. Kitsopoulos, C. J. Chick, Y. Zhao, and D. M. Neumark, J. Chem. Phys. **95**, 5479 (1991); C. C. Arnold, T. N. Kitsopoulos, and D. M. Neumark, *ibid.* (in press).
[17] T. N. Kitsopoulos, C. J. Chick, A. Weaver, and D. M. Neumark, J. Chem. Phys. **93**, 6108 (1990).
[18] For example, see K. J. Taylor, C. L. Pettiette, O. Cheshnovshy, and R. E. Smalley, J. Chem. Phys. **96**, 3319 (1992); J. Ho, K. M. Ervin, and W. C. Lineberger, *ibid.* **93**, 6987 (1990); J. G. Eaton, H. W. Sarkas, S. T. Arnold, K. M. McHugh, and K. H. Bowen, Chem. Phys. Lett. **193**, 141 (1992); G. Gantefor, M. Gausa, K. H. Meiwesbroer, H. O. Lutz, Faraday Discuss. Chem. Soc. **86**, 197 (1988); Z. Phys. D **9**, 253 (1988); S. M. Casey, P. W. Villalta, A. A. Bengali, G. L. Cheny, and D. G. Leopold, J. Am. Chem. Soc. **113**, 6688 (1991).
[19] L. S. Wang, J. Conceicao, C. M. Jin, and R. E. Smalley, Chem. Phys. Lett. **182**, 5 (1991); S. Yang, K. J. Taylor, M. J. Craycraft, J. Conceicao, C. L. Pettiette, O. Cheshnovsky, and R. E. Smalley, *ibid.* **144**, 431 (1988); C. C. Arnold, Y. Zhao, T. N. Kitsopoulos, and D. M. Neumark, J. Chem. Phys. **97**, 6121 (1992); D. W. Arnold, S. E. Bradforth, T. N. Kitsopoulos, and D. M. Neumark, *ibid.* **95**, 8753 (1991); T. N. Kitsopoulos, C. J. Chick, Y. Zhao, and D. M. Neumark, *ibid.* **95**, 5479 (1991).
[20] K. Müller-Dethlefs, M. Sander, and E. W. Schlag, Z. Naturforsch. Teil A **39**, 1089 (1984); Chem. Phys. Lett. **12**, 291 (1984); K. Müller-Dethlefs and E. W. Schlag, Ann. Rev. Phys. Chem. **42**, 109 (1991).
[21] E. P. Wigner, Phys. Rev. **73**, 1002 (1948).
[22] K. J. Reed, A. H. Zimmerman, H. C. Andersen, and J. I. Brauman, J. Chem. Phys. **64**, 1368 (1976).
[23] T. N. Kitsopoulos, I. M. Waller, J. G. Loeser, and D. M. Neumark, Chem. Phys. Lett. **159**, 300 (1989); T. N. Kitsopoulos, C. J. Chick, Y. Zhao, and D. M. Neumark, J. Chem. Phys. **95**, 1441 (1991).
[24] T. G. Dietz, M. A. Duncan, D. E. Powers, and R. E. Smalley, J. Chem. Phys. **74**, 6511 (1981).
[25] D. Proch and T. Trickl, Rev. Sci. Instrum. **60**, 713 (1989).
[26] C. C. Arnold, Y. Zhao, T. N. Kitsopoulos, and D. M. Neumark, J. Chem. Phys. **97**, 6121 (1992).